Thermal evolution of the crystal structure of the orthorhombic perovskite $LaFeO_3$

Charlotte A.L. Dixon, Christopher M. Kavanagh, Kevin S. Knight, Winfried Kockelmann, Finlay D. Morrison, Philip Lightfoot

www.elsevier.com/locate/yjssc

PII: S0022-4596(15)30071-2
DOI: http://dx.doi.org/10.1016/j.jssc.2015.07.019
Reference: YJSSC18992

To appear in: *Journal of Solid State Chemistry*

Received date: 29 May 2015
Revised date: 9 July 2015
Accepted date: 13 July 2015

Cite this article as: Charlotte A.L. Dixon, Christopher M. Kavanagh, Kevin S Knight, Winfried Kockelmann, Finlay D. Morrison and Philip Lightfoot, Therma evolution of the crystal structure of the orthorhombic perovskite $LaFeO_3$, *Journa of Solid State Chemistry,* http://dx.doi.org/10.1016/j.jssc.2015.07.019

Thermal evolution of the crystal structure of the orthorhombic perovskite $LaFeO_3$

Charlotte A. L. Dixon[1], Christopher M. Kavanagh[1], Kevin S. Knight[2], Winfried Kockelmann[2], Finlay D. Morrison[1] and Philip Lightfoot[1]*

1. School of Chemistry and EaStCHEM, University of St Andrews, St Andrews, KY16 9ST, UK.
2. ISIS Facility, Rutherford Appleton Laboratory, Chilton, Didcot, OX11 0QX, UK.

*E-mail **pl@st-and.ac.uk**; phone: +44-1334-463841; fax: +44-1334-463808

Abstract

The thermal evolution of the crystal structure of the prototypical orthorhombic perovskite $LaFeO_3$ has been studied in detail by powder neutron diffraction in the temperature range $25 < T < 1285$ K. A conventional bond length/bond angle analysis, combined with an analysis in terms of symmetry-adapted modes, allows key aspects of the thermal behavior to be understood. In particular, the largest-amplitude symmetry modes (*viz.* in-phase and out-of-phase octahedral tilts, and A-site cation displacements) are shown to display relatively 'normal' behavior, increasing with decreasing temperature, which contrasts with the anomalous behavior previously shown by the derivative $Bi_{0.5}La_{0.5}FeO_3$. However, an unexpected behavior is seen in the nature of the *intra*-octahedral distortion, which is used to rationalize the unique occurrence of a temperature dependent crossover of the *a* and *c* unit cell metrics in this compound.

Keywords: $LaFeO_3$; perovskite; symmetry mode analysis; powder neutron diffraction

Introduction

The series of lanthanide orthoferrites $LnFeO_3$ have been widely studied for a variety of physical and chemical properties, for example magnetism[1], multiferroicity[2], catalysis[3] and application in solid-oxide fuel cells[4]. This family also represents a very rich source of information for understanding trends in fundamental perovskite crystallography as a function of A-cation size[5,6]. For all lanthanides, the thermodynamically stable phase for $LnFeO_3$ at room temperature is the prototypical orthorhombically-distorted perovskite

(space group *Pnma*) represented by the Glazer tilt system $a^+b^-b^-$ (equivalently in this space group setting, $a^-b^+a^-$). This structure type is often known as 'the $GdFeO_3$ structure', or 'the *Pnma* perovskite' or '*Pbnm* perovskite', depending on the choice of axis system. The octahedral tilting gives rise to an enlarged unit cell, of four times the volume relative to the aristotype cubic perovskite cell a_p, given by $a_O \sim \sqrt{2}\ a_p$, $b_O \sim 2\ a_p$, $c_O \sim \sqrt{2}\ a_p$ in the standard *Pnma* setting (Figure 1). This is the most common distorted structure type for perovskites, and is typically stable for a range of tolerance factors[7], $t < 0.975$; the tolerance factor for $LaFeO_3$ is 0.954. As shown by Woodward[8], a balance of favorable covalent versus ionic bonding interactions at the A-site is largely responsible for the stability of this particular distortion, and for $0.975 < t < 1.02$ the alternative tilt system $a^-a^-a^-$ (described in space group *R*-3*c*) becomes more stable. This transition from *Pnma* to *R*-3*c* can be seen at room temperature, as a function of A-cation size in the series $LnNiO_3$[9] and also occurs as a function of increasing temperature in a number of perovskites, including $LaGaO_3$[10], $LaCrO_3$[11] and $LaFeO_3$ itself[12,13]. In this respect, an alternative view of the relative stabilities of the two structure types has been given in terms of the relative polyhedral volume ratios of the perovskite AO_{12} and BO_6 sites[14,15] (ie. the A-site polyhedron expands more rapidly versus temperature than the B-site, thus stabilizing the *R*-3*c* phase at higher T).

We have recently analysed the thermal behavior of the crystal structure of an unusual member of the $GdFeO_3$-structure perovkite family, *viz.* $Bi_{0.5}La_{0.5}FeO_3$ (BLFO)[16]. This compound was studied as a comparison to the important multiferroic perovskite $BiFeO_3$, which we had shown to undergo a transition to a paraelectric, but unstable, $GdFeO_3$-like structure at its ferroelectric T_C[17]. Our study of BLFO revealed some unexpected features; in particular a strong magnetostrictive effect below its magnetic ordering temperature, T_N, which leads to a highly unusual structural response. The primary aim of the present study was therefore to compare the behavior of BLFO to that of $LaFeO_3$, which has a similar T_N, a similar *t*, but a 'simpler' composition at the perovskite A-site, free from the effects of mixed cation influences, and the effects of the Bi^{3+} lone-pair. Powder neutron diffraction (PND) is the technique of choice for this study, as precise determination of light atom (oxygen) positions and also magnetic ordering are required.

Another structural curiosity in the $GdFeO_3$-structure perovkites is the observation of Zhou and Goodenough[6] that there is an inherent octahedral *distortion* present in this family, in addition to the octahedral tilting, which can rationalise subtle features in the evolution of lattice parameters for a given $LnMO_3$ family, as a function of Ln^{3+} size. In general for this Glazer tilt system, the relationship $a > c$ (in the *Pnma* setting) must always be valid, *if* the tilted octahedral units are perfectly rigid (since the a^- tilts occur around the *a*-axis of the orthorhombic unit cell). However, there are a few cases where $c > a$ occurs, and this is apparently due to the subtle octahedral distortions (specifically the deviation of the O-B-O angles in the *ac* plane away from 90°). Woodward et al.[18] suggest that deviation need only be of the order of 1° to over-ride the effect of a modest octahedral tilt on the relative *a/c* dimensions. The cases where $c > a$ are situated at the extreme end of the phase stability region of the *Pnma* phase ($t \geq 0.97$) and include $LaGaO_3$[10], $LaCrO_3$[11] and $SrRuO_3$[19]. $LaFeO_3$ itself ($t = 0.96$) is just below this region and, although it exhibits a unit cell with $a > c$ at room temperature a crossover to $c > a$ has recently been observed at around 700 K in the powder X-ray diffraction (PXRD) study of Selbach *et al.*[13]. As far as we are aware this is the only instance where such a crossover has been observed in a perovskite system as a function of temperature rather than composition. However, the previous study did not offer a detailed rationale for this behavior, perhaps because PXRD is unable to determine sufficiently precise oxygen atom positions. The second aim of this study is therefore to understand the detailed nature of this crossover, in terms of the precise evolution of all the relevant structural parameters versus temperature.

Experimental Section

Synthesis: Polycrystalline $LaFeO_3$ was synthesised using a conventional mixed oxide solid-state route. Stoichiometric quantities of La_2O_3 and Fe_2O_3 were thoroughly ball-milled (1hr @ 600 rpm) and heated in an alumina crucible to 800 °C for 5 hrs. Subsequent regrinding and re-annealing at 1100 °C for 10 hrs led to the final product. Powder X-ray diffraction (Panalytical Empyrean diffractometer) was used to confirm

phase purity.

Neutron powder diffraction (NPD): Time-of-flight neutron powder diffraction experiments were conducted using the HRPD and GEM diffractometers at the ISIS neutron spallation source at the Rutherford-Appleton Laboratories. The polycrystalline samples (~3 g) were mounted in cylindrical vanadium cans. Data were collected at a range of temperatures between 25 K and 550 K (HRPD) and 525 K and 1285 K (GEM). Each scan was counted for 40 μAhr (HRPD) or 50 μAhr (GEM) incident proton beam (corresponding to ca. 75 min and 20 minutes, real-time, respectively).

Diffraction Data Analysis: All diffraction data were analyzed by Rietveld refinement using the General Structure Analysis System (GSAS) software package. Parameters refined included background coefficients, lattice parameters, profile coefficients, atomic positional coordinates, isotropic atomic displacement parameters and magnetic moment for the Fe^{3+} site. For HRPD refinements data from two detector banks were used, whereas four detector banks were used in the case of GEM. Models and refinement strategies were kept as self-consistent as possible given the differences between the two instruments. Isotropic refinement of all atoms was carried out for the *Pnma* phase, whereas anisotropic refinement was used for the *R*-3*c* phase. Given the limitations of deriving precise, fully anisotropic thermal parameters and dynamical information from powder diffraction data, it should be borne in mind that the results presented here represent a time and space average crystal structure. In addition to traditional analysis of structure evolution in terms of bond lengths and angles, we find it constructive to complement this with analysis in terms of symmetry-adapted normal modes, which de-correlate the effects of octahedral tilts and other distortions; this is implemented in the ISODISTORT suite[20].

Results

Thermal evolution of lattice metrics

For all temperatures in the range 25 < T < 1255 K the diffraction patterns displayed clear superlattice reflections at the pseudocubic M-point ($\boldsymbol{k}$ = ½, 0, ½) and X-point ($\boldsymbol{k}$ = 0, ½, 0) in addition to the R-point ($\boldsymbol{k}$ = ½, ½, ½). The group-theoretical analysis of Howard and

Stokes[21] (which simplifies the Glazer tilt classification into 15 unique models based on strictly rigid tilts) suggests four possible space groups compatible with the simultaneous presence of both in-phase (M-point) and out-of-phase (R-point) tilts. Of these, only the $a^-b^+a^-$ tilt system is compatible with the observed primitive orthorhombic crystal symmetry, which signifies the *Pnma* space group as an unambiguous choice, in the present case. At a temperature of 1270 K the M-point and X-point peaks had disappeared, and the lattice metrics were compatible with rhombohedral symmetry, demonstrating the phase transition to the *R*-3*c* phase, with no evidence of an intermediate phase. For the magnetic structure, a G-type antiferromagnetic order, with the moment constrained along the *c*-axis, was found to be satisfactory (Shubnikov symmetry Pn□ma□), although a slight canting of the moment has been confirmed previously[22]. At a temperature of ~760 K the peaks due to magnetic ordering tended to zero, as shown by the refined value of magnetic moment (Supplemental material); this is slightly higher than previous reports of T_N in the range 735 - 750 K[23,24].

The thermal evolution of lattice parameters within the *Pnma* regime is shown in Figure 2. Representative Rietveld fits and further details of refinements are provided in the Supplemental material[25]. The greatest degree of 'orthorhombic distortion' is observed at the lowest temperatures; at intermediate temperatures the normalized (pseudo-cubic) parameters tend to coalesce, and a crossover from $a > c$ to $c > a$ is seen around 770 K, above which there is a divergence of the lattice parameters prior to the rhombohedral phase being reached. We note that there is a systematic offset of the lattice parameters derived from the HRPD and GEM data. Hence the apparent anomalies seen around the region 500 – 600 K are artefacts of these differing systematic errors. This is unfortunate, but of no serious consequence to the overall trends we observe in either lattice parameters or other derived structural features discussed below.

Thermal evolution of bond lengths/angles and symmetry-adapted modes

In the *Pnma* crystal structure the B-site (Fe) lies on an inversion center, and so there are three independent Fe-O bond lengths, three independent O-Fe-O bond angles and two independent Fe-O-Fe bond angles for the two unique O sites (Figure 1). The behavior of

these parameters versus temperature is shown in Figures 3-5.

In the symmetry-mode approach the seven independent positional parameters of the *Pnma* structure are re-cast as seven distinct internal modes[26]: two octahedral 'tilts' (labelled M_3^+ and R_4^+), three octahedral distortions (M_2^+, X_5^+(O) and R_5^+(O)) and two A-site cation displacements (X_5^+(A) and R_5^+(A)). Of these, the M_3^+, R_4^+ and X_5^+(A) modes are often found to have the largest mode amplitudes in many *Pnma* perovskites (further details of the mode amplitude definitions is given in the Supplemental). The M_3^+ mode ('in-phase' or '+' tilt in Glazer notation) acts around the *b*-axis, whilst the R_4^+ mode ('out-of-phase' or '-' tilt) is effectively a tilt around the *a*-axis of the orthorhombic supercell, in the *Pnma* setting. We note at this stage that the M_3^+ tilt, acting alone, does not break the 4-fold symmetry down the *b*-axis, and permits the *a* and *c* axial metrics to remain equal, whereas the R_4^+ tilt *enforces* $c < a$ if rigid octahedra are to be retained.

Discussion

Octahedral tilting, distortion and the *a-c* crossover

The behavior of the lattice metrics is in good agreement with the powder XRD study of Selbach *et al.*[13]; in particular the minimum of orthorhombic distortion coincides closely with T_N in both studies. This, however, seems to be purely coincidental. In contrast, this behavior is markedly different to that observed for $Bi_{0.5}La_{0.5}FeO_3$[16], where a maximum in orthorhombicity is observed near T_N; this is discussed in more detail later. In the present case, there is no abrupt change in behavior of the lattice parameters around T_N, but instead a more gradual 'plateauing' of the *a*-parameter below this temperature, whereas the relative expansivities of the *b* and *c* axes remain very similar towards lower temperatures.

The relative expansivities of the unit cell axes are clearly influenced by the thermal evolution of both Fe-O bond lengths and *inter*-octahedral (Fe-O-Fe) and *intra*-octahedral (O-Fe-O) bond angles. As shown in Fig. 1, the Fe-O1 bond vector has its largest component along the *b*-axis, and the expansion of this bond can be seen to be primarily responsible for the change in the *b*-axis, as shown in Figures 2 and 3: ie. the Fe-O1 bond

increases by ~ 0.028 Å (from 2.005 to 2.033 Å) over the region 25 < T < 1240 K, corresponding to an increase in *b* of ~ 0.087 Å (from 7.850 to 7.937 Å). In contrast, the Fe-O2 bond lengths are relatively invariant with temperature, and the changes in the *a* and *c* axes are therefore driven largely by changes in the bond angles (or correspondingly, octahedral tilts and distortive modes).

A particularly interesting feature of $LaFeO_3$ is the crossover from $a > c$ to $c > a$, as a function of increasing temperature. As discussed in the Introduction, this effect can be considered as a 'competition' between the 'out-of-phase' octahedral tilt mode around the *a*-axis (R_4^+ mode) and the O2-Fe-O2' *intra*-octahedral distortion angle (Fig. 4), which influences features predominantly within the *ac* plane. As can be seen from the evolution of the tilt modes (Fig. 6) both tilts show a general reduction in amplitude from lower to higher temperatures, but the changes in M_3^+ are much larger than those in R_4^+ across the entire temperature range. Indeed, the changes in M_3^+ are larger than those in R_4^+ even at intermediate temperatures, and show an escalating reduction in amplitude towards zero at the transition into the R-3c phase (symmetry requirements dictate a first-order transition here). At the lower temperatures studied (T < 600 K) there is a plateauing in the amplitude of the R_4^+ tilt. These trends might suggest that an instability at the M-point is the primary driver for structural evolution, and that changes in the R-point tilt are secondary. The changes in the M_3^+ and R_4^+ tilt modes are mirrored in the corresponding *inter*-octahedral (Fe-O-Fe) angles, which show a smooth and large expansion for Fe-O2-Fe angle and a smaller change for Fe-O1-Fe, which plateaus at low temperature (Fig. 5). The O2-Fe-O2' angle shows quite a remarkable behavior. As can be seen in Fig. 4, the O2-Fe-O2' angle (largely 'in-plane' relative to the *a* and *c* axes) exhibits a near-constant value (~91.2°) across the entire temperature range, significantly deviating from the ideal 90°, but not subject to thermal variation. On the contrary, the O1-Fe-O2 and O1-Fe-O2' ('out-of-plane') angles show changes of similar magnitude (1.5 - 2°) but opposite sign across the temperature range studied. Hence, the crystal-chemical origin of the *a-c* crossover is clear, though perhaps surprising: it is driven by the fact that, across the key temperature range 600 < T < 900 K, the decreasing amplitude of the R_4^+ tilt allows *c* to increase relative to *a*, whereas the significant, but constant, in-plane distortion of the

FeO_6 octahedron, as defined by the O2-Fe-O2' angle, does not allow *a* to recover relative to *c* on approaching the higher temperature regime.

A-site modes and comparison to $Bi_{0.5}La_{0.5}FeO_3$

In addition to the octahedral tilt modes discussed above, there are five other internal degrees of freedom. Of these, the three relating to oxygen atoms only represent different distortions of the octahedral units; each of these is relatively small and/or relatively invariant with temperature (see Supplemental). In fact, the significant distortion (O2-Fe-O2') of the FeO_6 octahedron highlighted in the previous section is de-correlated from these internal modes, and is best perceived simply as a lattice strain: 'stretching' of the *c versus a* unit cell axes. The two remaining modes are the A-site (La^{3+}) cation displacements: X_5^+(A) is the most significant, and relates to an anti-polar displacement of successive *b*-axis layers along the *a*-axis (Fig. 1), whereas R_5^+(A) relates to a much smaller displacement along the *c*-axis. An interesting feature of the unit cell axial behaviour (Fig. 2) which we have not yet addressed, is the continuing divergence of the *a* and *c* axes towards lower temperature despite the fact that the R_4^+ mode no longer continues to increase below ~ 600 K. The reason for this is not straightforward to see in terms of any direct geometrical measure of the octahedral framework, but is almost certainly driven by the continually increasing displacement of the A-cation (principally *via* the X_5^+(A) mode below this temperature (Fig. 7). Typically, in the *Pnma* perovskite the two features of increased octahedral tilting and increased A-site displacement towards lower temperature are expected to go hand-in-hand. In this case, although the only tilt mode that is still increasing significantly towards lower T (ie. M_3^+) cannot directly affect the *c/a* ratio, it clearly still co-operates to allow the A-site displacement and consequently permits a mechanism that allows the *a*-axis to achieve a relatively low thermal expansivity at the lowest temperatures. It is well-known[8] that covalent contributions to the A-O bonding encourage the A-site displacements in this structure type, and bond-valence arguments[27,28] can be used to show that the resultant shorter/longer A-O bond distribution relative to the *a* rather than *c*-axis will allow this effective 'expansion' of *a* versus *c* at lower temperatures. In fact, the bond valence sum for La^{3+} does increase due

to the enhanced displacement (Supplemental), but apparently does not negate the above argument.

One of the original aims of this study was to compare the thermal structural response of this parent material to the more complex derivative BLFO. The latter material displays some highly unusual features in its structural behavior versus temperature[16]. In particular, the most significant macroscopic feature is a dramatic plateauing of the expansivity of the *c*-axis (not the *a*-axis) below T_N. This is ascribed to a magnetostrictive response to the antiferromagnetic ordering, which is correlated with counter-intuitive changes to both the M_3^+ and X_5^+(A) modes: ie. both the in-phase tilt mode and the A-site *a*-axis displacements *decrease* significantly throughout the temperature regime below T_N. The orthorhombic distortion in BLFO also shows a maximum near T_N, in contrast to the minimum seen here, and there is no *a*-*c* axis crossover. As we have seen above, there is no such magnetostrictive effect in $LaFeO_3$ (although we do observe a very small 'excess volume' effect, as described in the previous PXRD study[13]). Moreover, for $LaFeO_3$, the variation of the M_3^+ and X_5^+(A) modes proceeds in the intuitively expected sense, ie. larger amplitudes towards lower temperatures.

Obviously the differences in behavior must be due to the nature of the A-site occupancy: although La^{3+} and Bi^{3+} have nominally very similar ionic radii[23], their electronic nature is fundamentally different, Bi^{3+} displaying a stereochemically-active lone pair. These features are shown by a comparison of the unit cell volumes for the two, which are very similar throughout the temperature range studied. For example, at 300 K and 700 K: 242.8 and 245.5 $Å^3$ for $LaFeO_3$ and 243.6 and 246.2 $Å^3$ for BLFO, respectively. On the other hand the thermal evolution of both the individual cell parameters and also the key mode amplitudes are dramatically different. At 300 K the structure of $LaFeO_3$ is surprisingly similar to that of BLFO, with mode amplitudes M_3^+, R_4^+, X_5^+(A) of 0.719, 1.206, 0.321 and 0.744, 1.225 and 0.259 for $LaFeO_3$ and BLFO, respectively. The corresponding values at 700 K are: 0.658, 1.196, 0.268 for $LaFeO_3$ and 0.837, 1.167 and 0.313 for BLFO, emphasizing the contrasting trends in M_3^+ and X_5^+(A), in particular.

Conclusions

$LaFeO_3$ retains an orthorhombic (*Pnma*) perovskite structure across a very wide temperature range 25 < T < 1255 K, and is free from the complicating effects seen in other examples of this, the most common structural distortion of the perovskite structure (for example those having 'lone-pair' cations at the A-site or 'Jahn-Teller' cations at the B-site). This system therefore serves as an excellent model to understand the nature of some of the key structural distortions common to this structure type. Although a magnetic ordering transition occurs within the *Pnma* phase regime, this appears not to have any dramatic magneto-structural influence, in contrast to that seen in the Bi-containing derivative $Bi_{0.5}La_{0.5}FeO_3$. Nevertheless, a curious anisotropic thermal expansion is observed in $LaFeO_3$, and this has been rationalized in detail using both conventional geometric arguments and complementary symmetry-mode analysis. Several significant features are highlighted, some of which are unexpected: anisotropic bond length expansion, differing behavior of the two octahedral tilt modes and an invariant O-Fe-O bond angle. The latter effect is shown to be the key influence in understanding the previously reported crossover of the *a* and *c* parameters in this composition, and further emphasizes that although 'rigid octahedral tilts' provide an essential starting point for the analysis of perovskite structures, more subtle effects must also be taken into account in explaining some of the more esoteric structural behaviors encountered.

Supplementary Material

Representative CIF files (for Rietveld refinements at 50, 275, 775, 1210 and 1270 K) have been deposited with ICSD: further details may be obtained from Fachinformationszentrum (FIZ) Karlsruhe, 76344 Eggenstein-Leopoldshafen, Germany (e-mail: crysdata@fiz-karlsruhe.de) on quoting deposition numbers 429714-429718.

Acknowledgements

We thank STFC for provision of neutron diffraction facilities at ISIS. CALD and CMK were supported by EPSRC DTA studentships.

References

1. K. Ueda, H. Tabata and T. Kawai, Science, **280** (1998) 1064.
2. Y. Tokunaga, N. Furukawa, H. Sakai, Y. Taguchi, T. H. Arima, and Y. Tokura, Nature Mater., **8** (2009) 558.
3. A. E. Giannakas, A. K. Ladavos and P. J. Pomonis, Appl. Catal. B, **49** (2004) 147.
4. K. Huang, H. Y. Lee and J. B. Goodenough, J. Electrochem. Soc., **145** (1998) 3220.
5. M. Marezio, J. P. Remeika and P. D. Dernier, Acta Cryst., **B26** (1970) 2008.
6. J.-S. Zhou and J. B. Goodenough, Phys. Rev. Lett., **94** (2005) 065501.
7. V. M. Goldschmidt, Naturwiss., **21** (1926) 477. (The Goldschmidt tolerance factor relates the lengths of the A-O and B-O bonds *via*: $t = [(<(A\text{-}O)>/\sqrt{2} <(B\text{-}O)>])$.
8. P. M. Woodward, Acta Cryst., **B53** (1997) 44.
9. P. Lacorre, J. B. Torrance, J. Pannetier, A. I. Nazzal, P. W. Wang, and T. C. Huang, J. Solid State Chem., **91** (1991) 225.
10. K. S. Knight, J. Solid State Chem., **194** (2012) 286.
11. K. Oikawa, T. Kamiyama, T. Hashimoto, Y. Shimojyo and Y. Morri, J. Solid State Chem., **154** (2000) 524.
12. S. Geller, and P. M. Raccah, Phys. Rev. B, **2** (1970) 1167.
13. S. M. Selbach, J. R. Tolchard, A. Fossdal, and T. Grande, J. Solid State Chem., **196** (2012) 249.
14. M. Avdeev, E. N. Caspi and S. Yakovlev, Acta Cryst., **B63** (2007) 363.
15. D. Wang and R. J. Angel, Acta Cryst., **B67** (2011) 302.
16. C. M. Kavanagh, R. J. Goff, A. Daoud-Aladine, P. Lightfoot and F. D. Morrison, Chem. Mater., **24** (2012) 4563.
17. D. C. Arnold, K. S. Knight, F. D. Morrison and P. Lightfoot, Phys. Rev. Lett., **102** (2009) 027602.
18. P. M. Woodward, T. Vogt, D. E. Cox, A. Arulraj, C. N. R. Rao, P. Karen and A. K. Cheetham, Chem. Mater., **10** (1998) 3652.

19. C. W. Jones, P. D. Battle, P. Lightfoot and W. T. A. Harrison, Acta Cryst., **C45** (1989) 365.
20. B. J. Campbell, H. T Stokes, D. E. Tanner and D. M. Hatch, J. Appl. Cryst., **39** (2006) 607.
21. C. J. Howard and H. T. Stokes, Acta Cryst., B54 (1998) 782.
22. T. Peterlin-Neumaier and E. Steichele, J. Magn. Magn. Mater., **59** (1986) 351.
23. S. Stølen, F. Grønvold, H. Brinks, T. Atake and H. Mori, J. Chem. Thermodynamics, **30** (1998) 365.
24. W. C. Koehler and E. O. Wollan, J. Phys. Chem. Solids, **2** (1957) 100.
25. See Supplemental material at xxxxxxx.
26. K. S. Knight, Canad. Miner., **47** (2009) 381.
27. R. D. Shannon, Acta Cryst., **A32** (1976) 751.
28. I. D. Brown, Acta Cryst., **B48** (1992) 553.

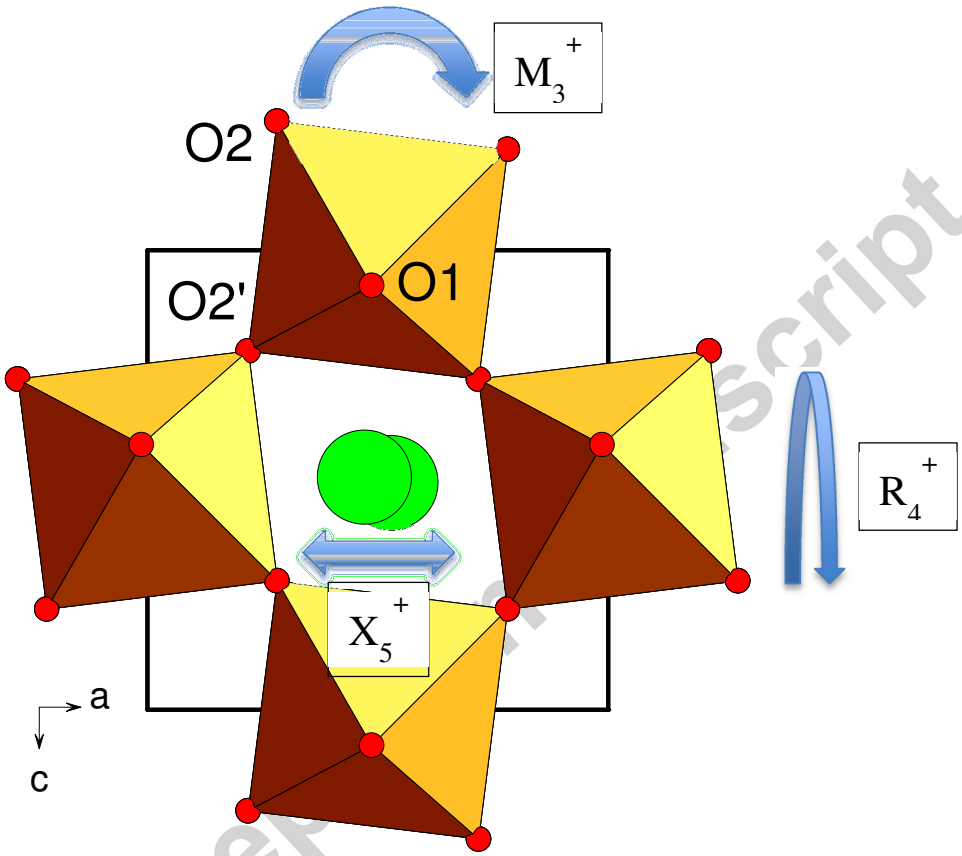

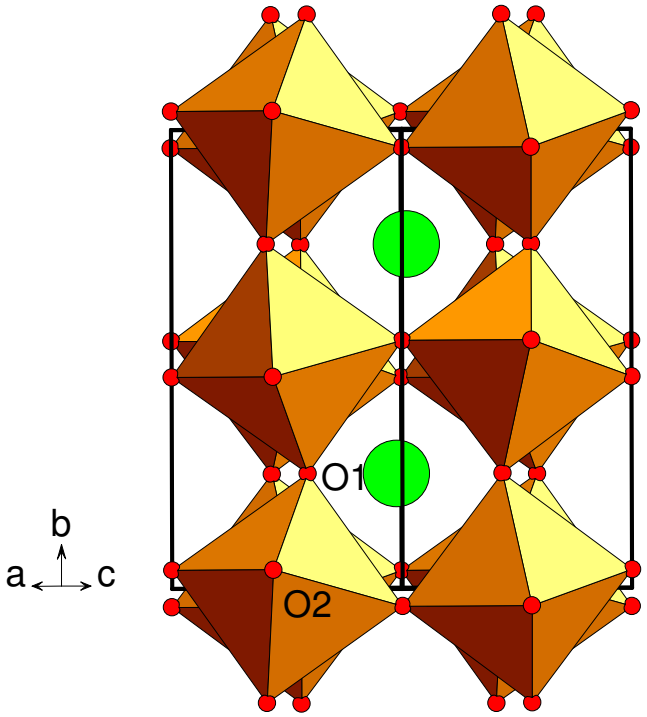

Figure 1. Crystal structure of $LaFeO_3$ viewed along (a) [010] and (b) [101]. The principal tilt modes and A-site displacive mode are shown schematically.

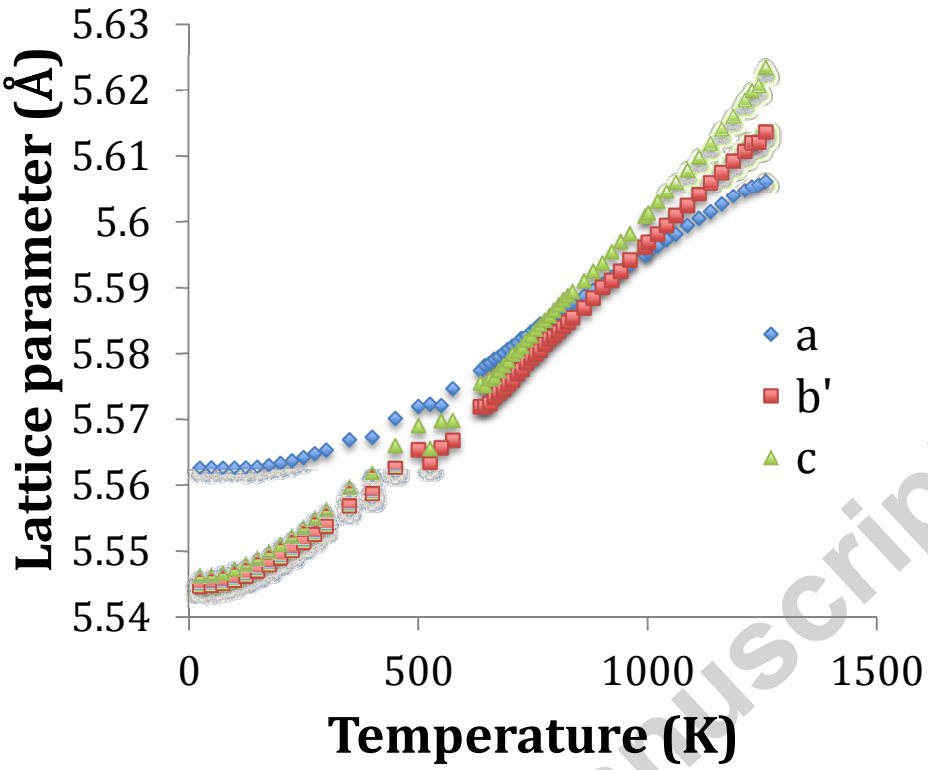

Figure 2. Thermal evolution of the lattice parameters. Note that $b' = b/\sqrt{2}$

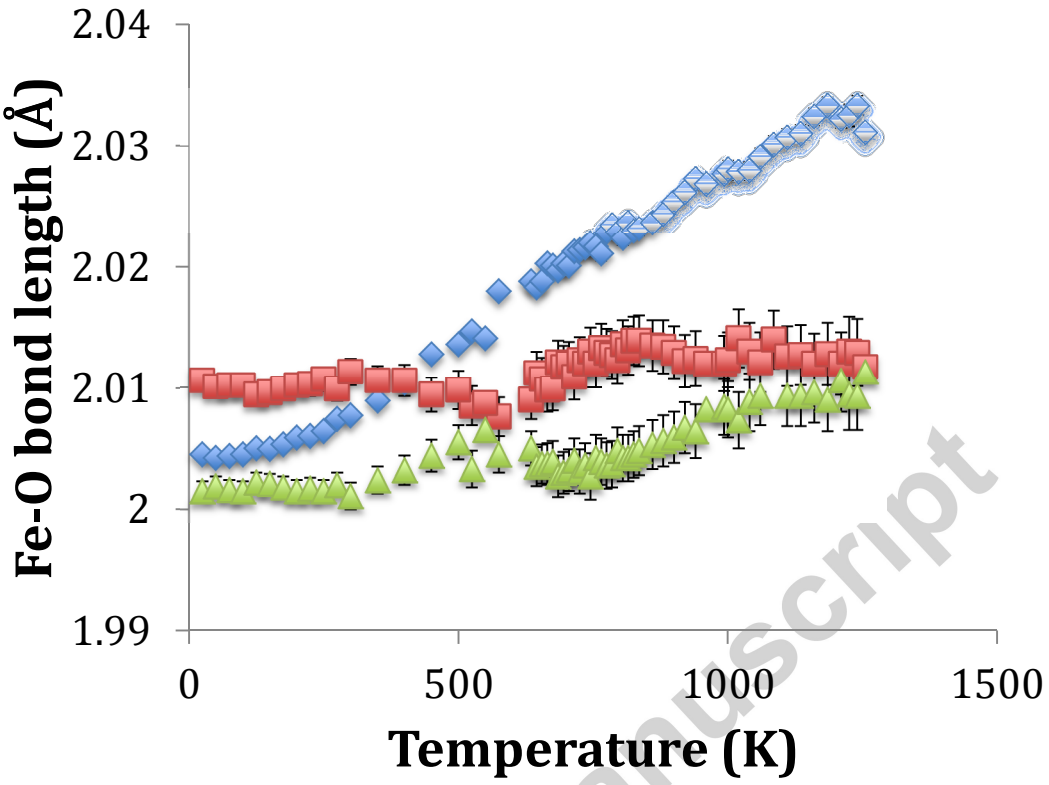

Figure 3. Thermal evolution of the Fe-O bond lengths: Fe-O1 (diamonds), Fe-O2 (triangles), Fe-O2' (squares).

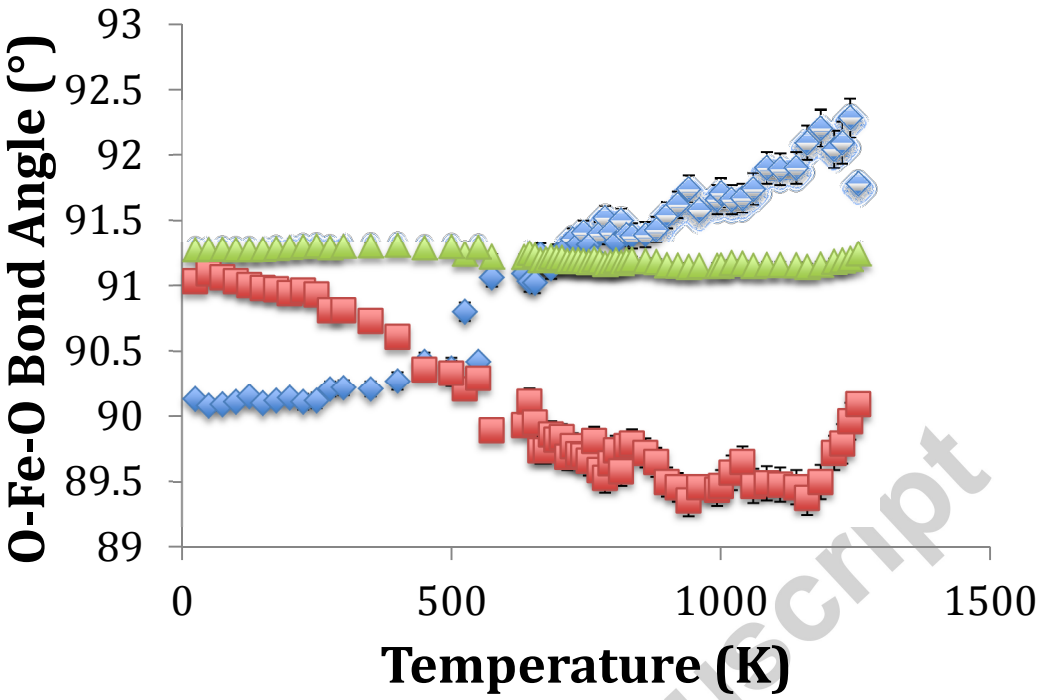

Figure 4. Thermal evolution of the O-Fe-O bond angles: O2-Fe-O2' (triangles), O1-Fe-O2 (squares), O1-Fe-O2' (diamonds).

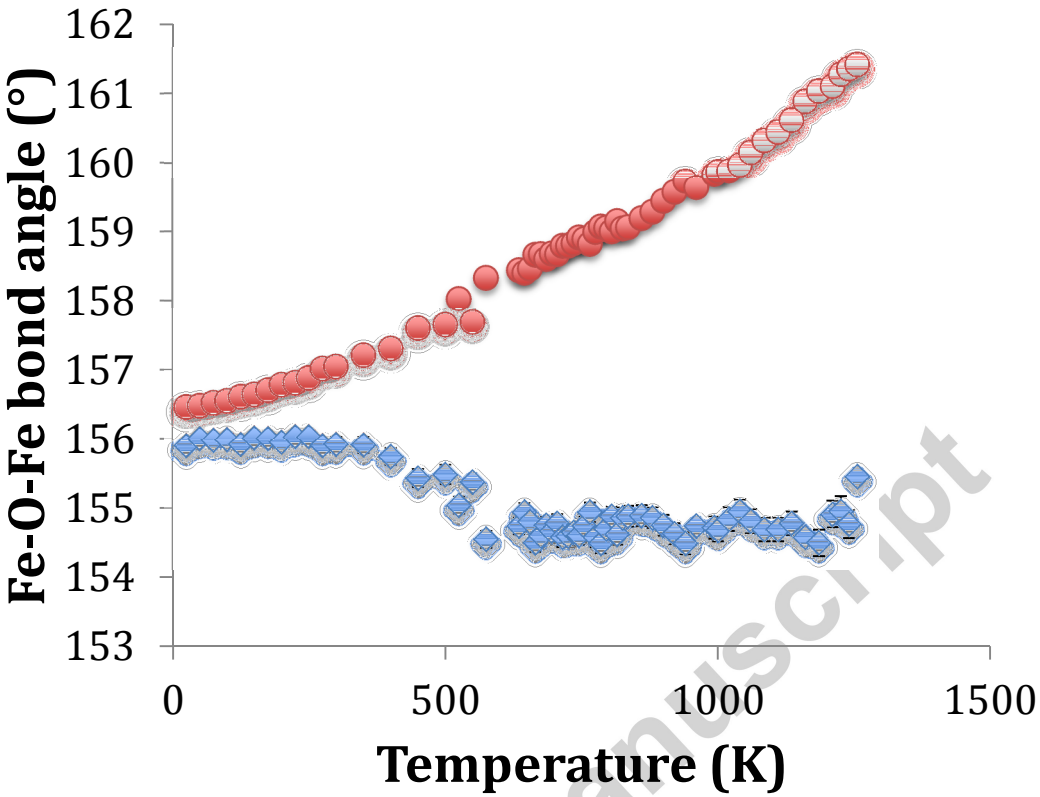

Figure 5. Thermal evolution of the Fe-O-Fe bond angles: Fe-O1-Fe (diamonds), Fe-O2-Fe (circles).

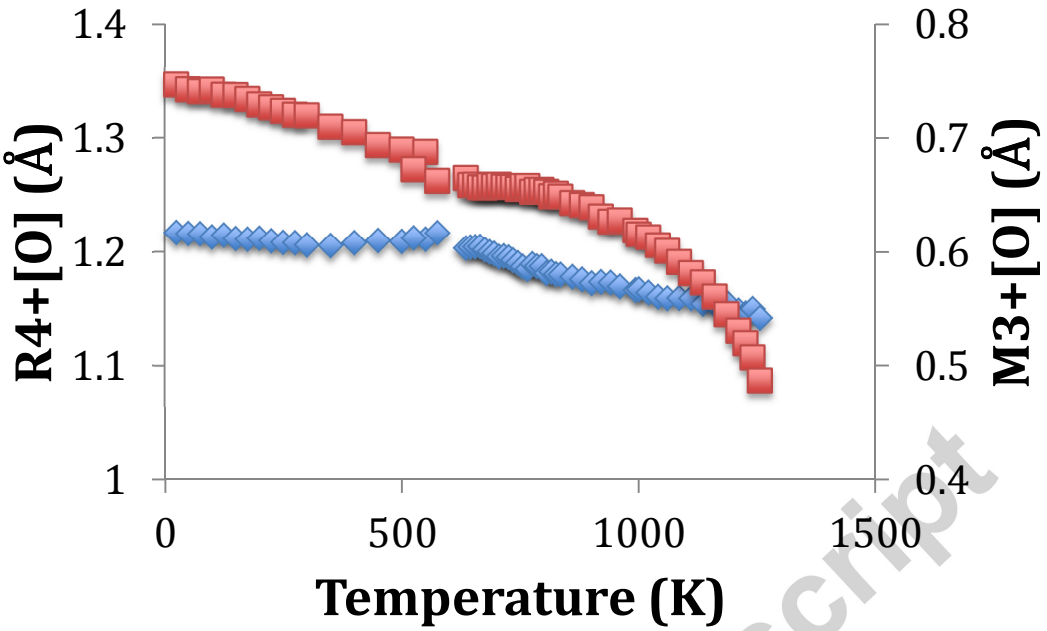

Figure 6. Thermal evolution of octahedral tilt modes: M_3^+ (squares), R_4^+(diamonds).

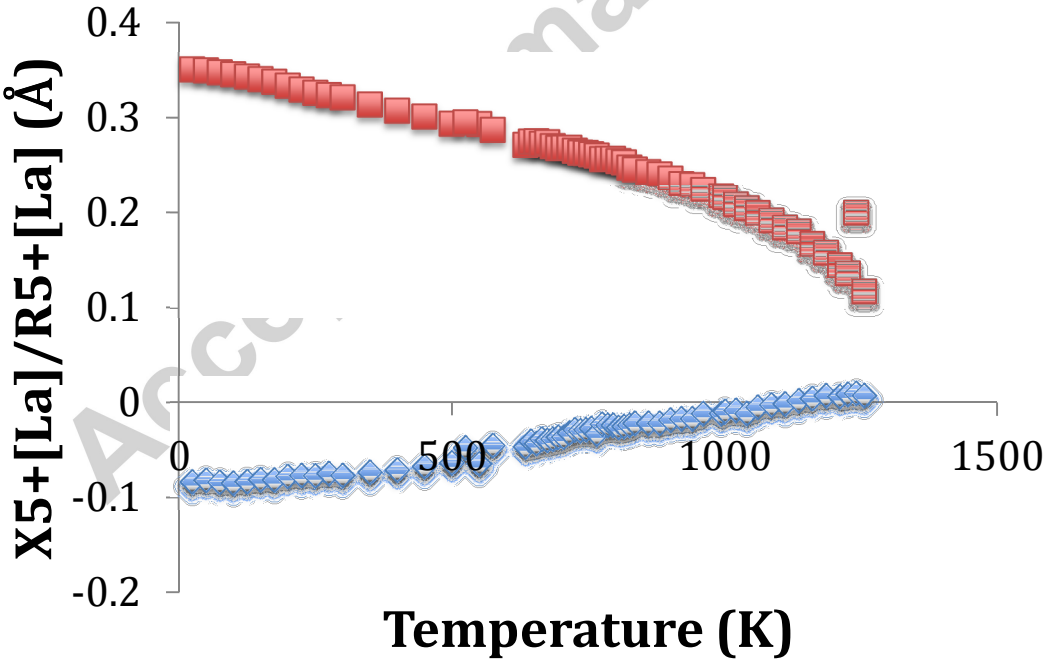

Figure 7. Thermal evolution of the A-site displacive modes: X_5^+ (squares), R_5^+ (diamonds).

Graphical Abstract

The unusual thermal evolution of lattice metrics in the perovskite $LaFeO_3$ is rationalised from a detailed powder neutron diffraction study.

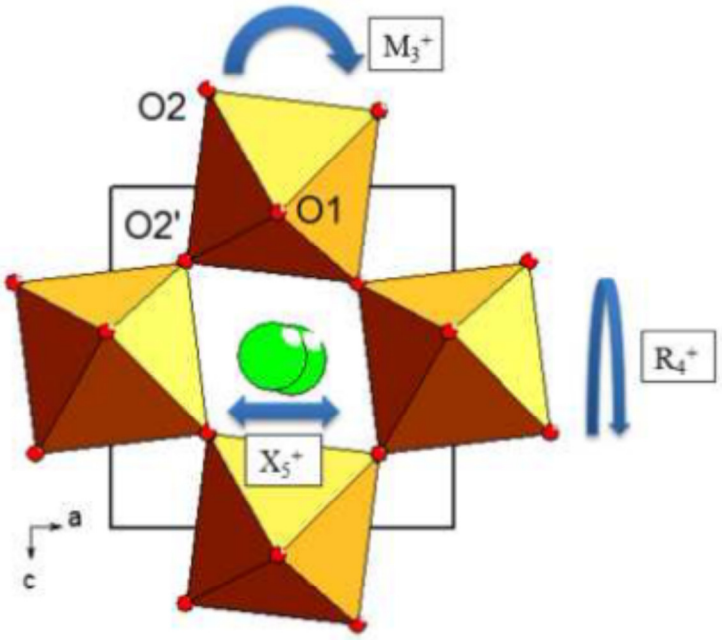

Highlights

Crystal structure of the perovskite $LaFeO_3$ studied in detail by powder neutron diffraction.
Unusual thermal evolution of lattice metrics rationalised.
Contrasting behaviour to Bi-doped $LaFeO_3$.
Octahedral distortion/tilt parameters explain unusual *a* and *c* lattice parameter behaviour